

Parametric Studies of Kinetically-Enhanced Raman Backscatter and Electron Acoustic Thomson Scattering

D. J. Strozzi¹, E. A. Williams¹, A. B. Langdon¹, A. Bers²

¹*Lawrence Livermore National Laboratory, Livermore, CA 94550, USA*

²*Massachusetts Institute of Technology, Cambridge, MA 02139, USA*

Work at LLNL performed under the auspices of the U.S. Department of Energy by University of California, Lawrence Livermore National Laboratory under Contract W-7405-Eng-48.

UCRL-POST-221801

Poster Tu08
36th Anomalous Absorption Meeting
Jackson Hole, Wyoming
6 June 2006

Abstract

Recent experiments^{1,2} and simulations^{3,4} show stimulated Raman backscatter (SRBS) in regimes of heavy Landau damping significantly above linear levels. This kinetic enhancement is attributed to electron trapping, which reduces Landau damping and downshifts the plasmon frequency. Experiments also measure reflected light between the SRBS and pump laser wavelengths, which has been interpreted as stimulated electron acoustic scattering (SEAS) off an electron acoustic wave (EAW).

We present Vlasov-Maxwell simulations with the Eulerian code ELVIS⁵ which show kinetic enhancement of SRBS and electron acoustic scattering (EAS), for an intermediate range of pump strengths. Once SRBS is enhanced, beam acoustic modes (BAMs) and an electron acoustic wave (EAW) are seen. The observed EAS phase-matches with a point on the EAW curve, but the EAW is mostly energized well below this frequency. EAS is a Thomson-like scattering off a separately-generated EAW. We call this process electron acoustic Thomson scattering (EATS).

We propose the beam acoustic decay (BAD) mechanism for energizing the EAW. Namely, the SRBS plasmon parametrically decays to another BAM and an EAW. Since the daughter BAM-to-EAW energy ratio is much greater than expected from Manley-Rowe, BAD may be a two-pump process, where the daughter BAMs are excited another way and beat with the SRBS plasmon to produce EAWs. The rest of the EAW curve is weakly excited by harmonic generation, which provides fluctuations to Thomson scatter the pump.

We study the linear modes of simulation distribution functions by projection onto a Hermite-Gauss basis. The resulting modes include a heavily-damped EAW and a series of BAMs, some of which are linearly unstable for certain k ; this may cause their excitation. These modes match the simulation electrostatic spectrum. Bispectral analysis further supports our BAD-EATS picture.

The physics of kinetic enhancement and EATS is similar both in low-density, low-temperature single-hot-spot regimes, as well as high-temperature, high-density hohlraum fill regimes.

¹D. S. Montgomery et al., *Phys. Plasmas* **9**, 2311 (2002); ²J. L. Kline et al., *Phys. Rev. Lett.* **94**, 175003 (2005);

³H. X. Vu et al., *Phys. Rev. Lett.* **86**, 4306 (2001); ⁴L. Yin et al., *Phys. Rev. E* **73**, 025401 (2006);

⁵D. J. Strozzi et al., *J. Plasma Phys.*, accepted 2005

Motivation: single-hot-spot experiments (Trident) show enhanced SRBS and stimulated (?) electron acoustic scatter (SEAS)

enhanced SRBS:

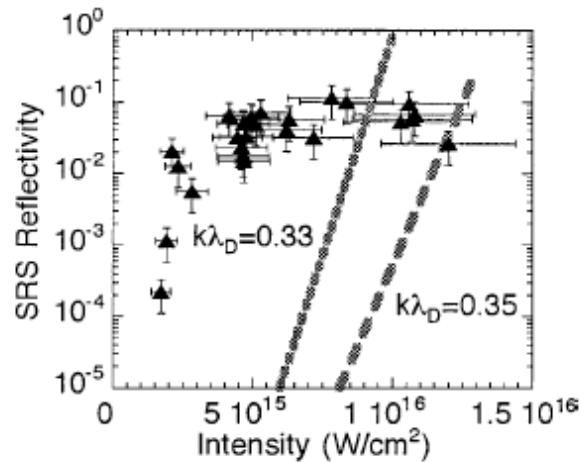


FIG. 5. Peak SRS reflectivity versus laser intensity for plasma conditions $k\lambda_D \sim 0.33-0.35$. The dashed lines show predictions from the SRS steady-state model for this range of conditions. The linear SRS model severely underestimates reflectivities in this regime, from which we infer lower than classical damping.

SEAS:

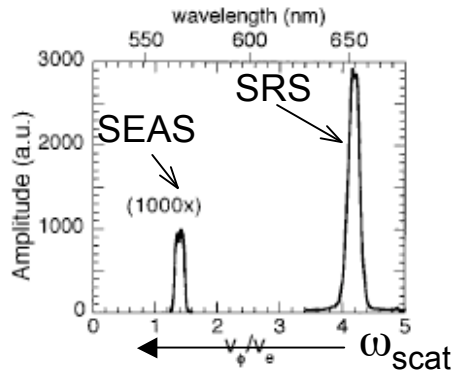


FIG. 9. Plot of SEAS and SRS backscatter spectrum vs electrostatic wave v_ϕ/v_e for single hot spot experiment. SEAS mode is shown 1000× larger. Upper axis corresponds to the scattered light wavelength.

LDI vs trapping:

lower k

higher k

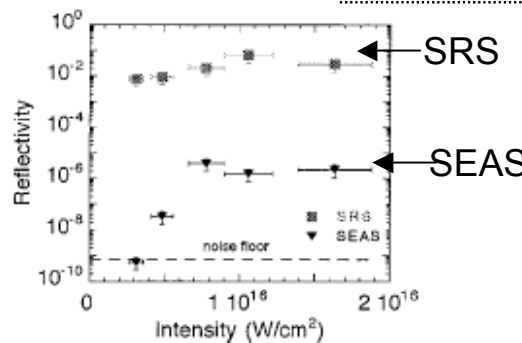


FIG. 10. Plot of measured reflectivity in SRS and SEAS vs laser intensity. SEAS reflectivity drops below detection level for $I \lesssim 3 \times 10^{15}$ W/cm², and is $\sim 3000\times$ below the SRS levels for higher intensity.

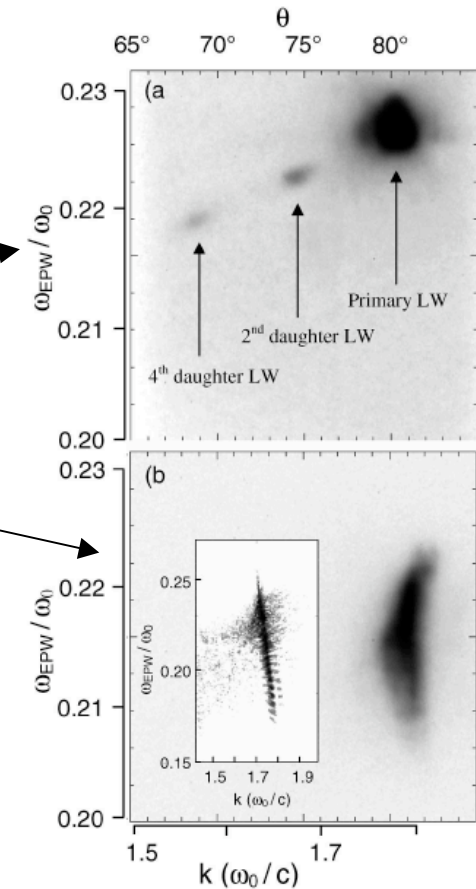


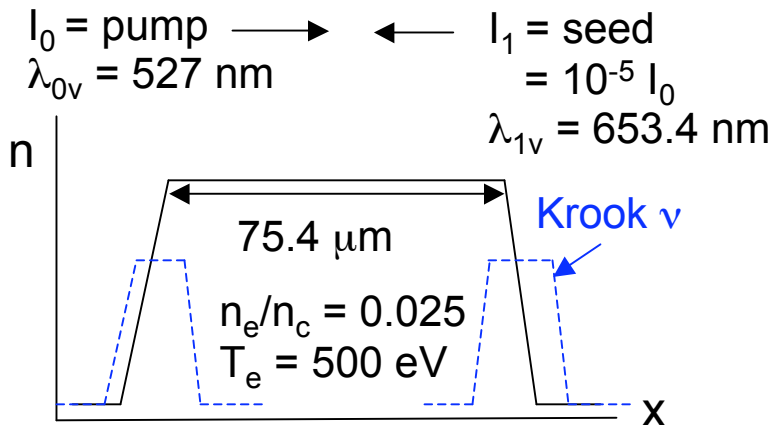
FIG. 3. Thomson scattering LW (ω, k) spectrum for (a) $k\lambda_D \sim 0.29$ showing the primary SRS LW and two copropagating LDI daughter LWs and for (b) $k\lambda_D \sim 0.34$ in the kinetic regime showing a broad frequency spectrum with a narrow wave-number spectrum. The inset in (b) shows a PIC simulation at $k\lambda_D = 0.30$ in which the (ω, k) spectrum is broad in ω and narrow in k , qualitatively consistent with the measurement. Electron trapping is observed in phase space for the simulation.

[D. S. Montgomery et al., *Phys. Plasmas* **9**, 2311 (2002)]

[J. L. Kline et al, *Phys. Rev. Lett.* **94**, 175003 (2005)]

ELVIS Vlasov simulations: SRBS bursty, kinetically enhanced above linear gain level

“Trident” Parameters

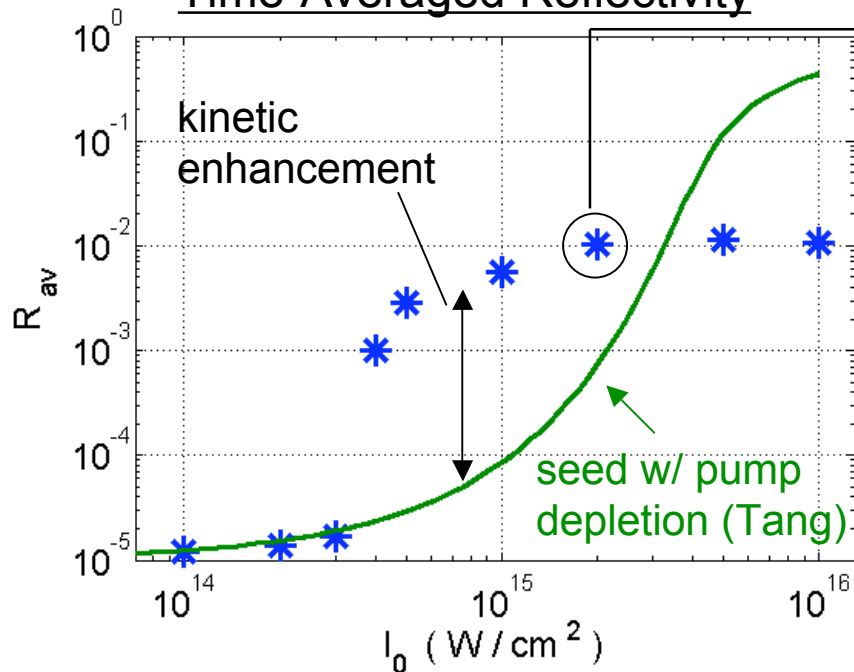


Simulations with 1-D Eulerian Vlasov-Maxwell solver ELVIS; fixed ions.
 [D. J. Strozzi et al., *J. Plasma Phys.*, accepted 2005;
 D. J. Strozzi et al., *Comput. Phys. Comm.* **164**, 156 (2004)]

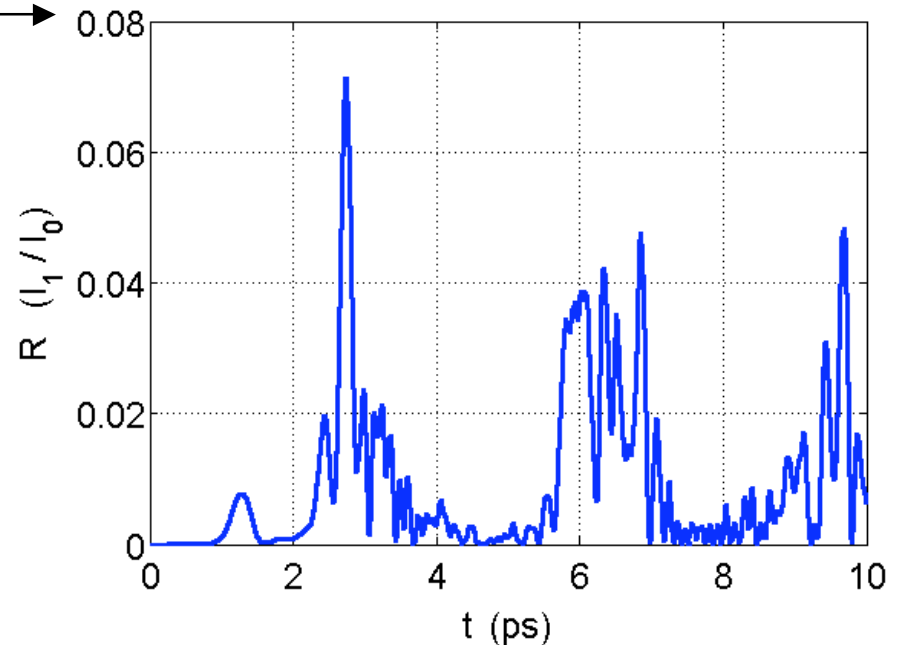
$$I_0 = 2 \cdot 10^{15} \text{ W/cm}^2$$

linear matching: EPW $k_2 \lambda_D = 0.352$
 amp. gain rate = $0.0289 \mu\text{m}^{-1}$,
 intensity gain = 4.36, $R_{av} = 7.81 \cdot 10^{-4}$

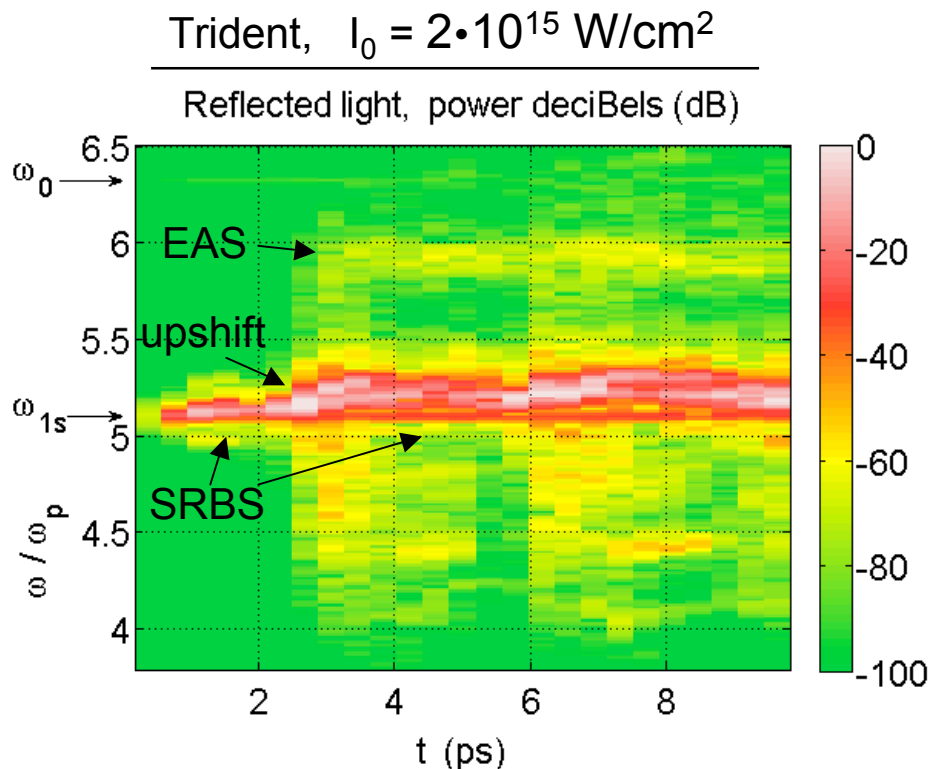
Time-Averaged Reflectivity



simulation $R_{av} = 1.03\%$



Reflected light: SRBS upshifts due to electron trapping; electron acoustic scatter (EAS) develops after kinetic enhancement

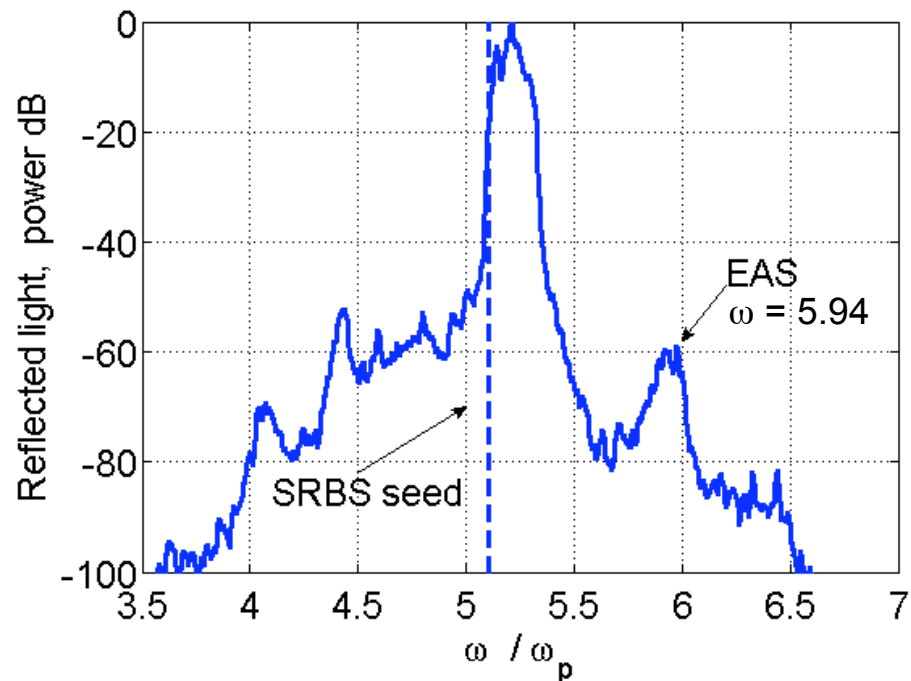


Electron trapping in Raman plasmon reduces Landau damping, gives kinetic enhancement.

Trapping also downshifts the plasmon frequency, which upshifts scattered light.

[T. O'Neil, *Phys. Fluids* **8**, 2255 (1965);
 G. J. Morales and T. M. O'Neil, *Phys. Rev. Lett.* **28**, 417 (1972);
 H. X. Vu et al., *Phys. Rev. Lett.* **86**, 4306 (2001)]

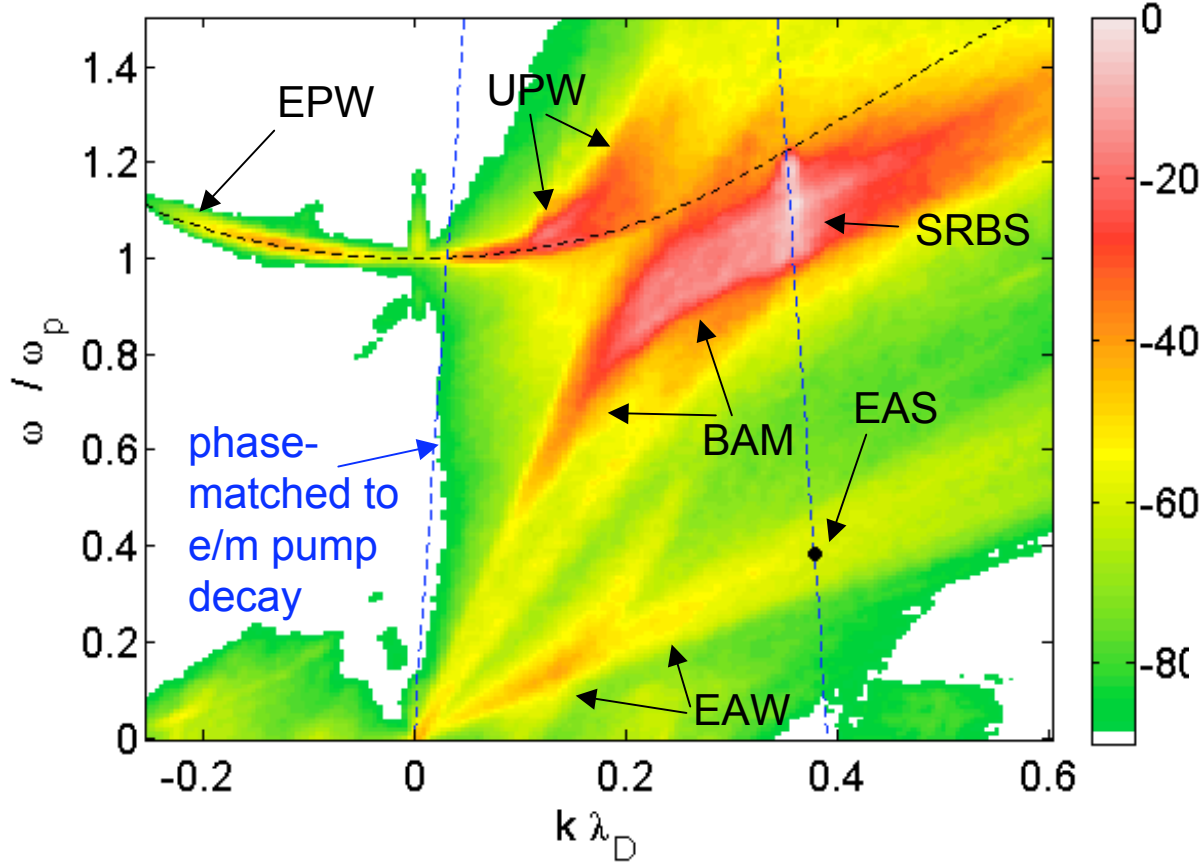
Time-integrated spectrum



Electrostatic spectrum shows plasmon downshift, electron acoustic waves

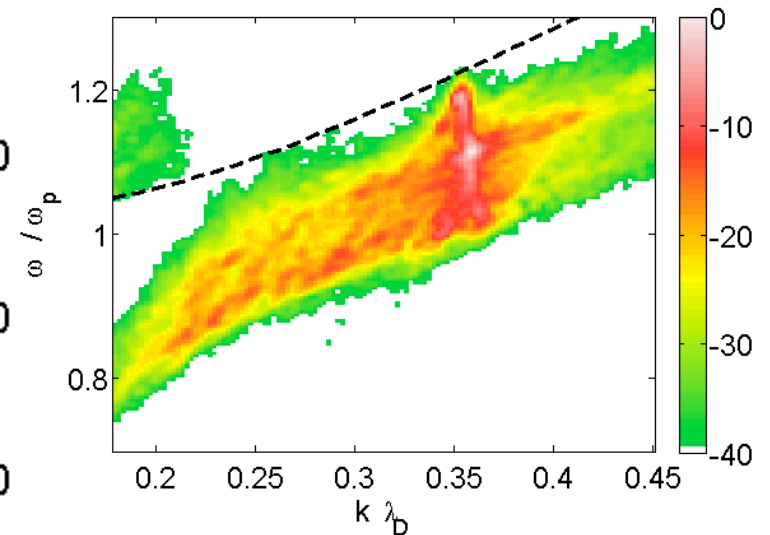
$$I_0 = 2 \cdot 10^{15} \text{ W/cm}^2$$

E_x , power dB



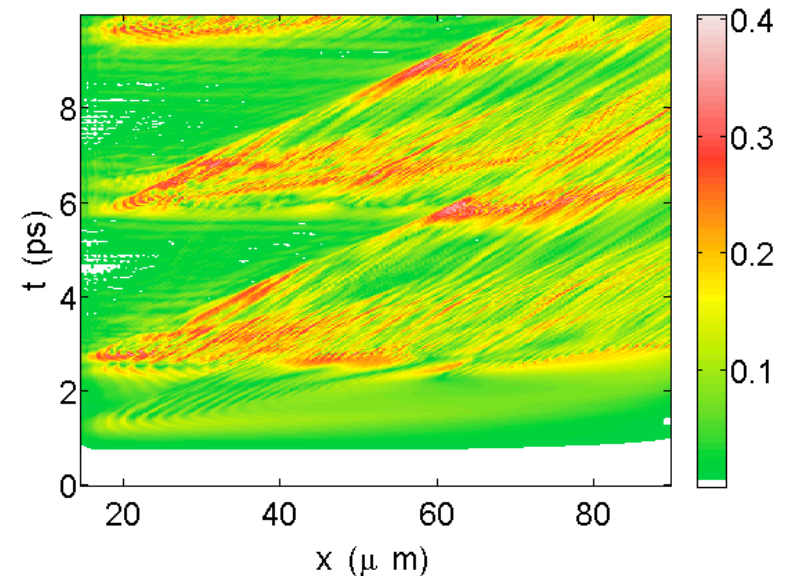
SRBS streak (zoomed)

E_x , power dB



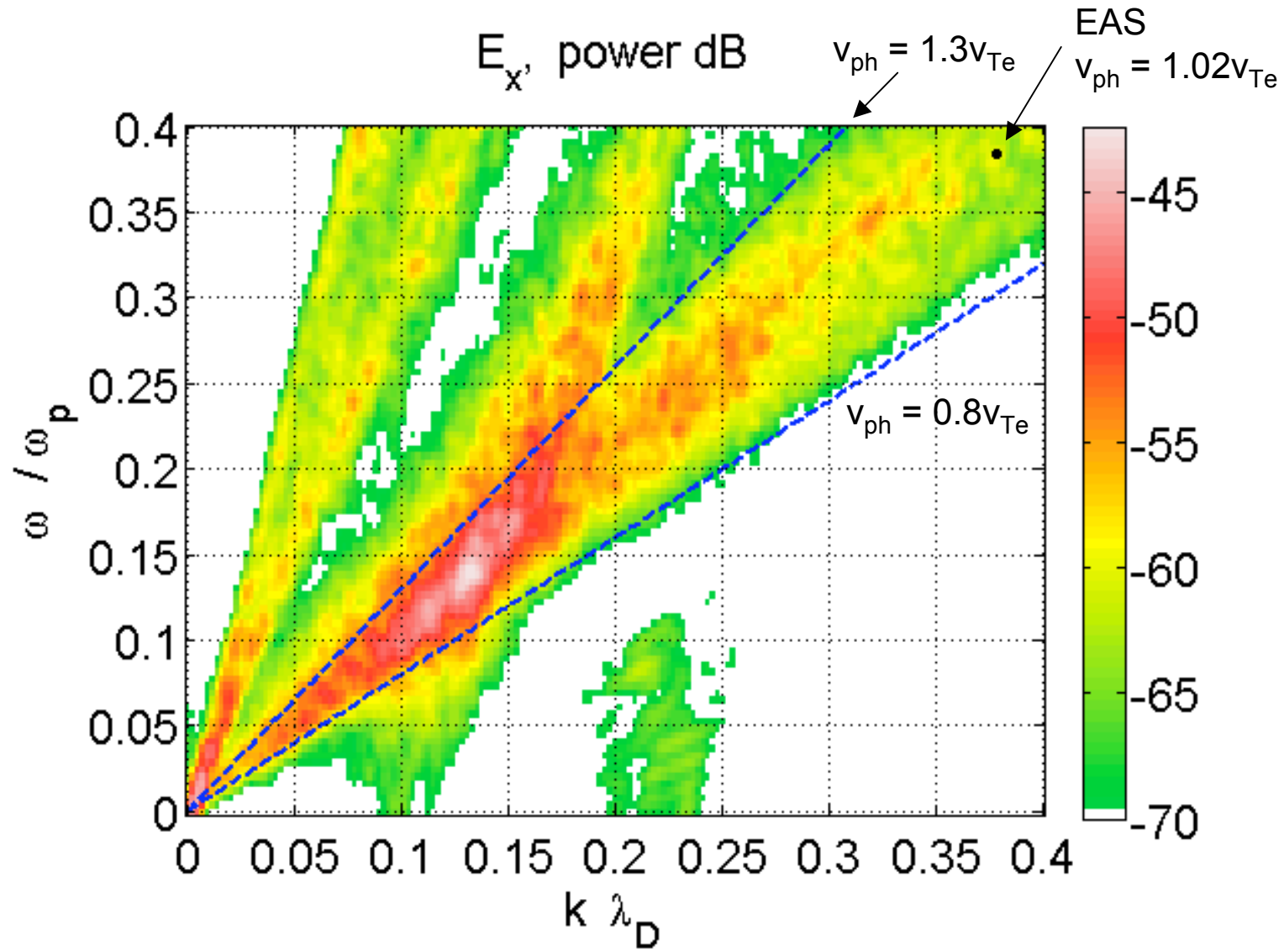
electrostatic envelope

rms $E_x (\epsilon_0 / (n_e T_e))^{1/2}$



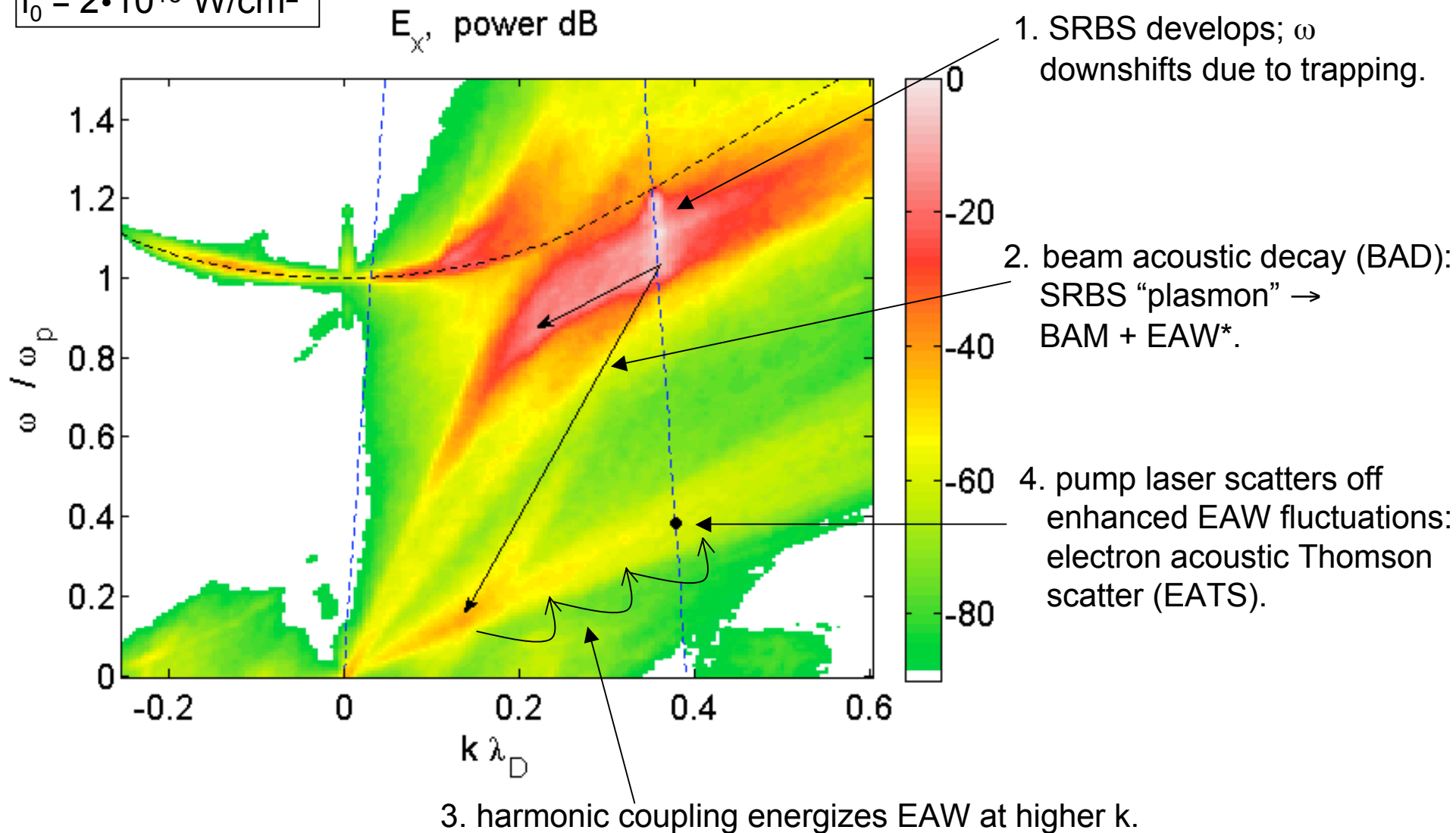
- SRBS plasmon downshifts in ω due to trapping.
- Linear EPW curve 'splits' into two branches.
- Beam acoustic modes (BAMs) observed, similar to L. Yin et al., *Phys. Rev. E* **73**, 025401 (2006).
- Electron acoustic waves (EAWs) excited mostly for $k \lambda_D < 0.2$, well below EAS matching point.

Electron acoustic wave (EAW) strongest well below EAS matching frequency



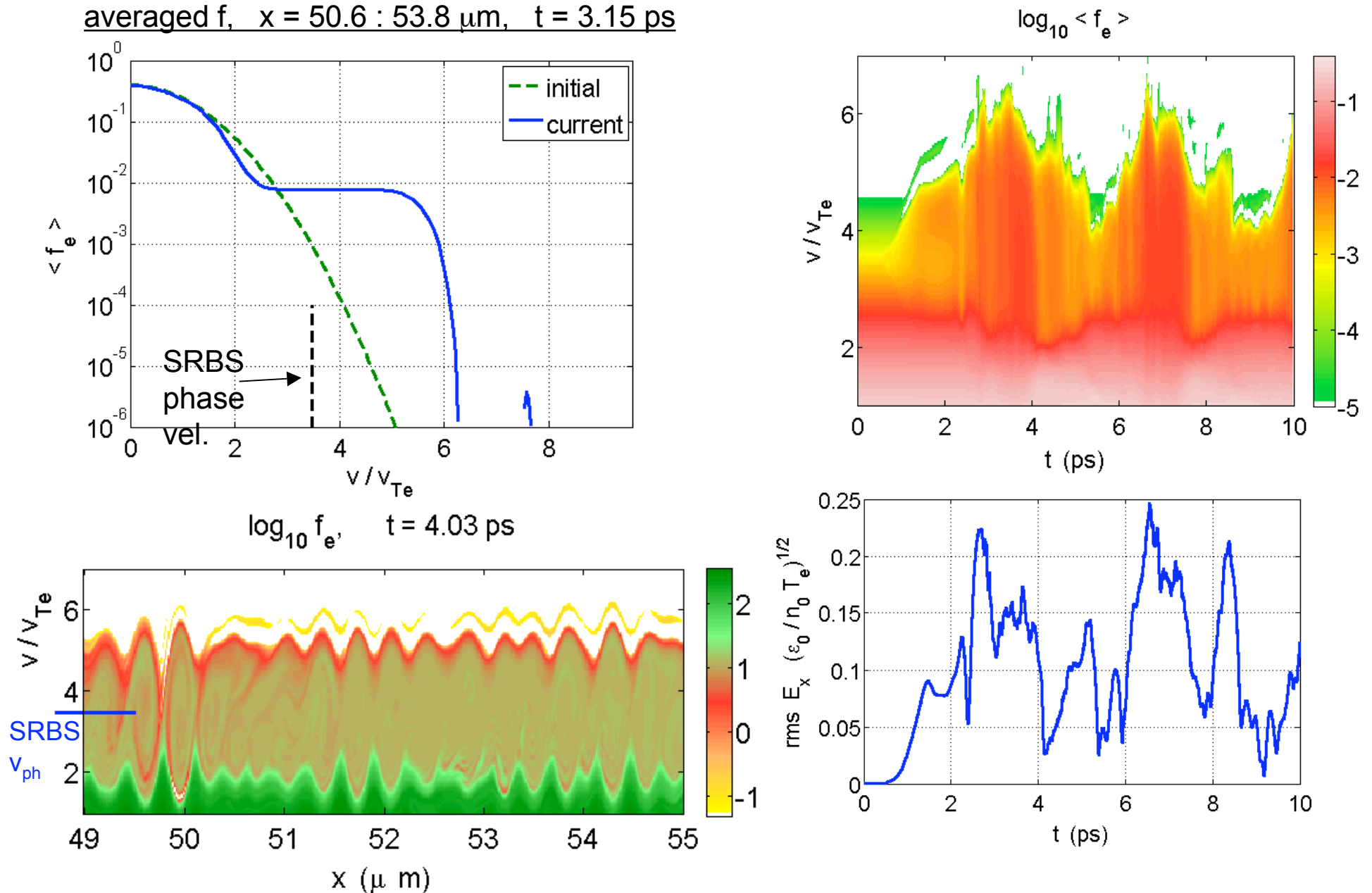
Beam acoustic decay (BAD) - electron acoustic Thomson scatter (EATS) picture

$$I_0 = 2 \cdot 10^{15} \text{ W/cm}^2$$



*Displayed BAD involves an EAW with phase velocity $1.14 v_{Te}$

Distribution function shows vortices and persistent flattening, roughly tied to wave amplitude ($I_0 = 2 \cdot 10^{15} \text{ W/cm}^2$)



Hermite projection yields linear modes of arbitrary distribution

$$\chi(v_p) = -k^{-2} \chi_v(v_p) \quad \chi_v(v_p) = \frac{d}{dv_p} \int dv \frac{f}{v - v_p} \quad \omega_{pe} = \lambda_{De} = v_{Te} = 1$$

$$v_p = \omega/k$$

•Hermite projection:

$$f(v) = \sum_{n=0}^N f_n \phi_n(v) \quad \phi_n(v) = \frac{1}{\pi^{1/4} \sqrt{2^n n!}} H_n(v) \exp(-v^2/2) \quad f_n = \int_{-\infty}^{\infty} dv \phi_n(v) f(v)$$

$$\chi_v(v_p) = \sum f_n \chi_{vn}(v_p) \quad \chi_{vn}(v_p) = \frac{d}{dv_p} \int dv \frac{\phi_n(v)}{v - v_p}$$

•Recurrence relation:

$$\chi_{vn} = - \left(\frac{2}{n} \right)^{1/2} \chi'_{v,n-1} + \left(\frac{n-1}{n} \right)^{1/2} \chi_{v,n-2}, \quad n \geq 2$$

$$\chi_{v0} = \frac{\pi^{1/4}}{\sqrt{2}} Z'(v_p/\sqrt{2}) \quad \chi_{v1} = -\frac{\pi^{1/4}}{\sqrt{2}} Z''(v_p/\sqrt{2})$$

•Upshot:

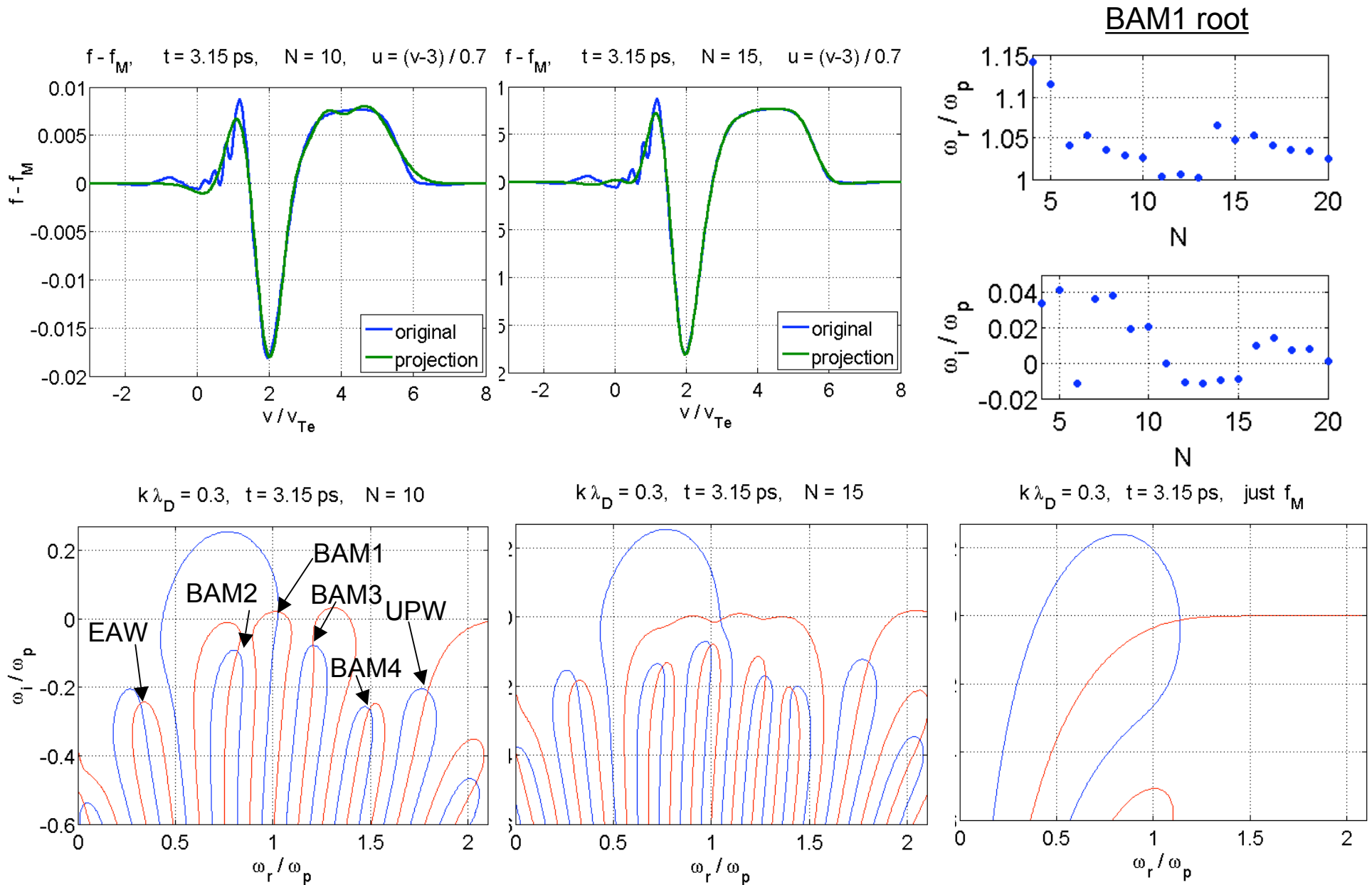
$$\chi_{vn}(v_p) = P_{Z,n+1}(v_p) Z(v_p/\sqrt{2}) + P_{R,n}(v_p)$$

$P_{Z,n}, P_{R,n} =$
Nth order polynomials

Advantages of projection vs. numerical integration for χ :

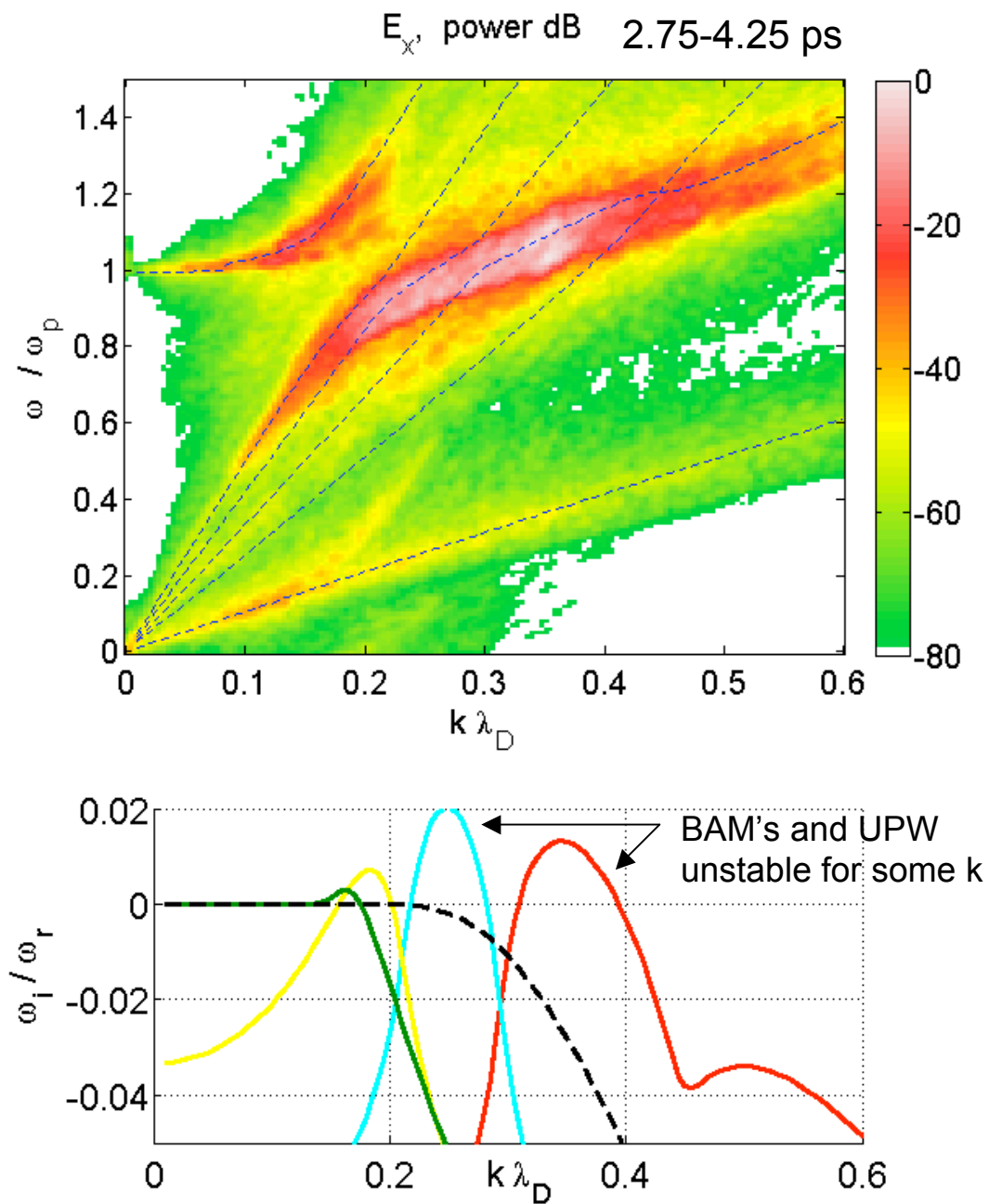
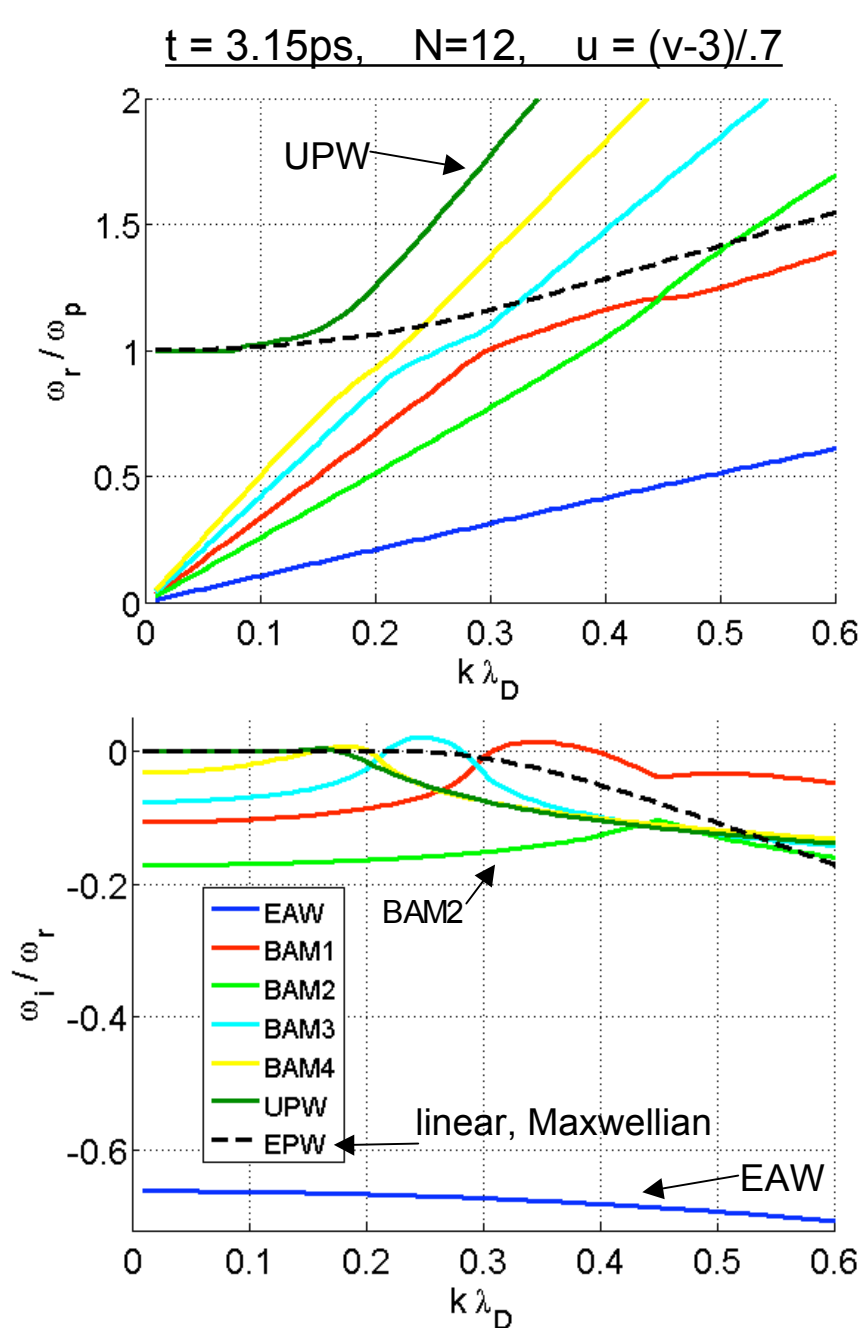
- Analytic form: faster to evaluate given a good Z function routine
- Complex plane: Landau contour, analytic continuation handled via Z function
- Easy to use in complex root finder (e.g. Newton's method)

Hermite method reveals roots absent for Maxwellian ($I_0 = 2 \cdot 10^{15} \text{ W/cm}^2$)

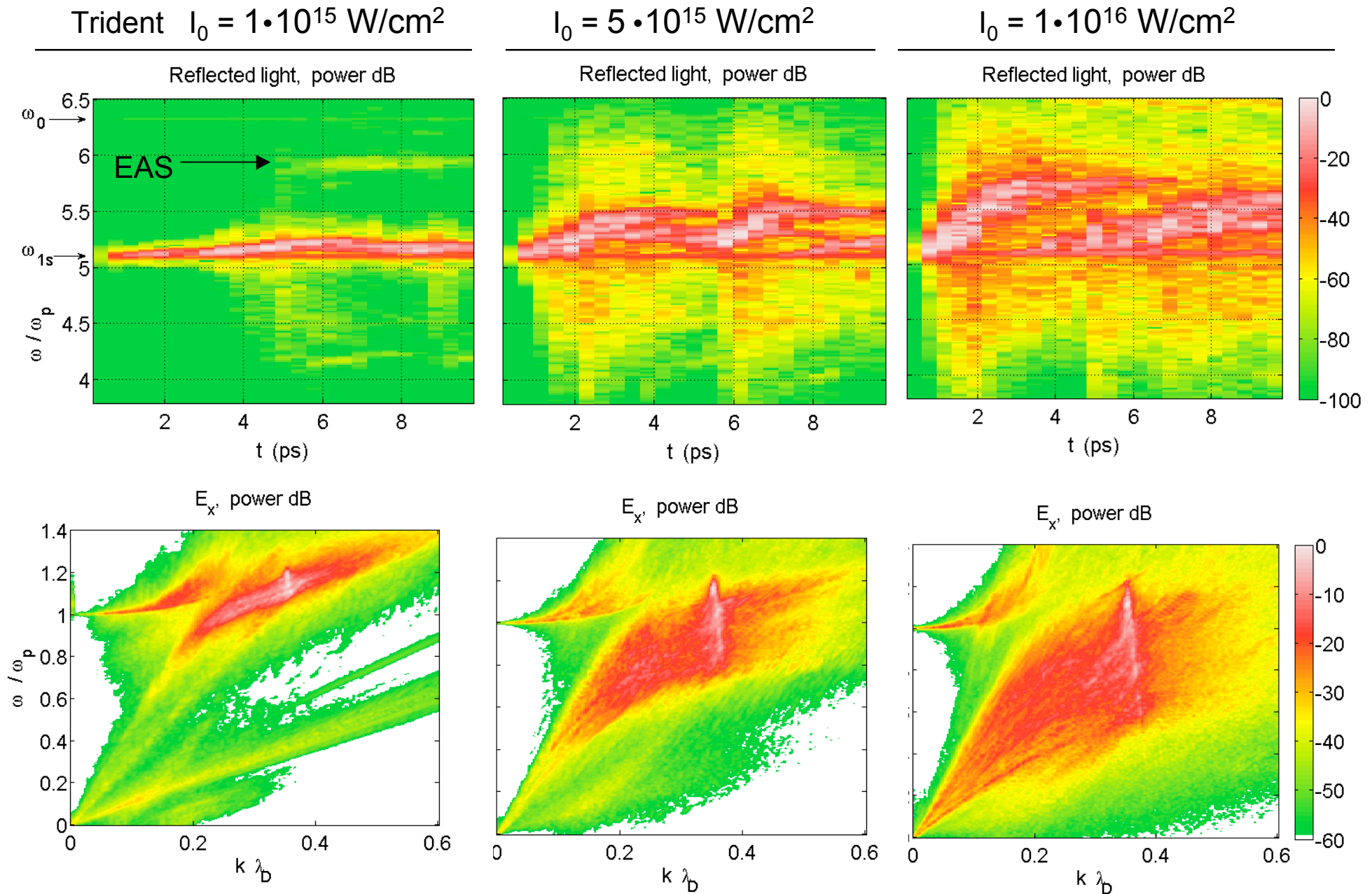


N choice: consider turning point of N^{th} basis function compared to support of $f - f_M$.

Roots vs. k agree with observed electrostatic spectrum ($I_0 = 2 \cdot 10^{15} \text{ W/cm}^2$)



At higher intensities, frequency shifts are very large; EAS not distinct



Bispectral analysis measures phase-locked signals that satisfy frequency-matching

x, y, z = real; stationary; zero mean: cumulants = moments through 3rd order

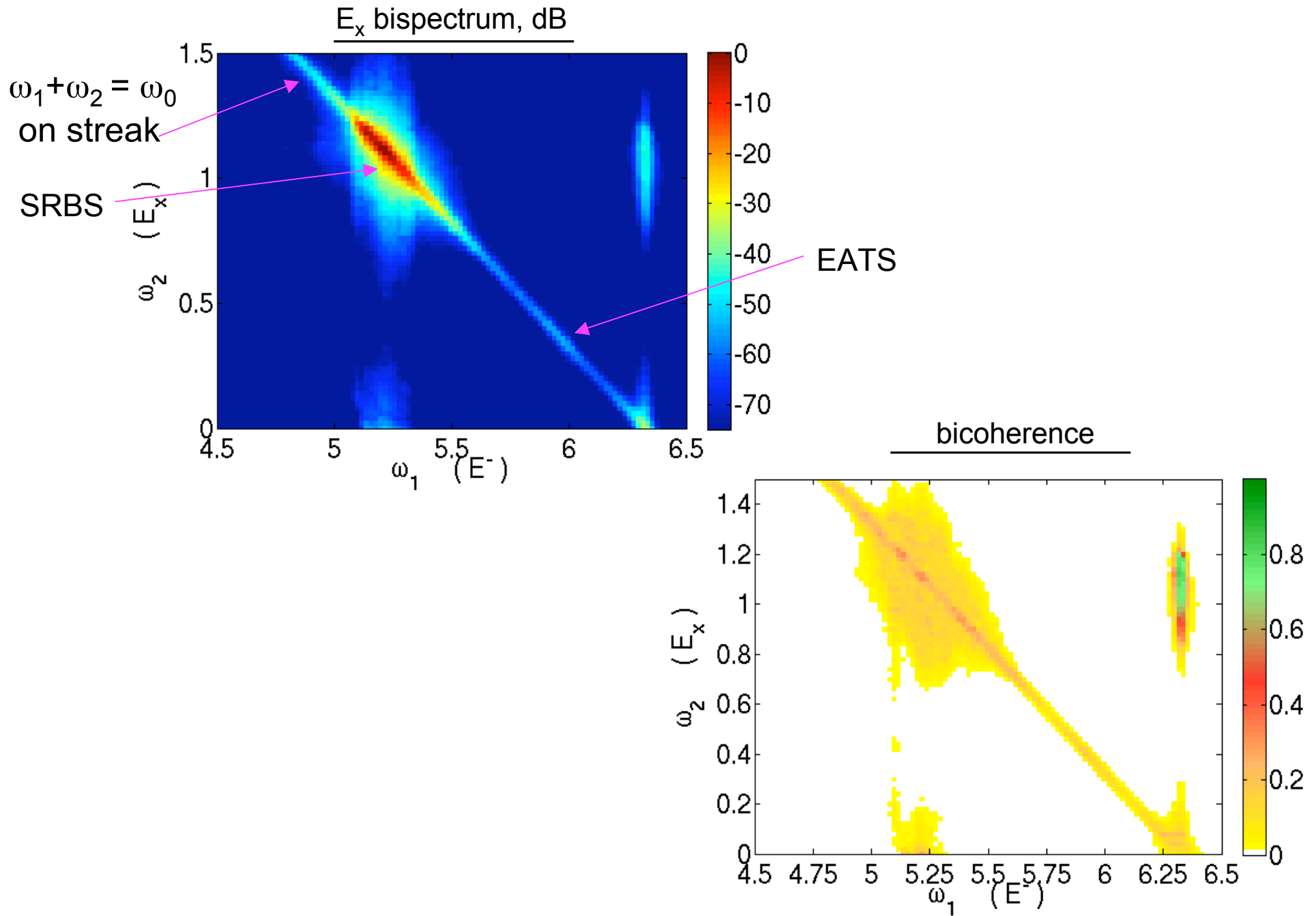
- 2-point correlation (order 2 cumulant): $C_2(\tau) = \frac{1}{2T} \int_{-T}^T dt x(t)y(\tau + t)$
- Power spectrum (Wiener-Khinchin): $P_2(\omega) = \int_{-\infty}^{\infty} d\tau e^{-i\omega\tau} C_2(\tau) = \langle X^*(\omega)Y(\omega) \rangle$
- 3-point correlation function: $c_3(\tau_1, \tau_2) = \frac{1}{2T} \int_{-T}^T dt x(t)y(\tau_1 + t)z(\tau_2 + t)$
- bispectrum:
(complex; phase info): $P_3(\omega_1, \omega_2) = \int_{-\infty}^{\infty} d\tau e^{-i(\omega_1\tau_1 + \omega_2\tau_2)} C_3(\tau_1, \tau_2)$

$$P_3(\omega_1, \omega_2) = \langle X^*(\omega_1 + \omega_2)Y(\omega_1)Z(\omega_2) \rangle$$

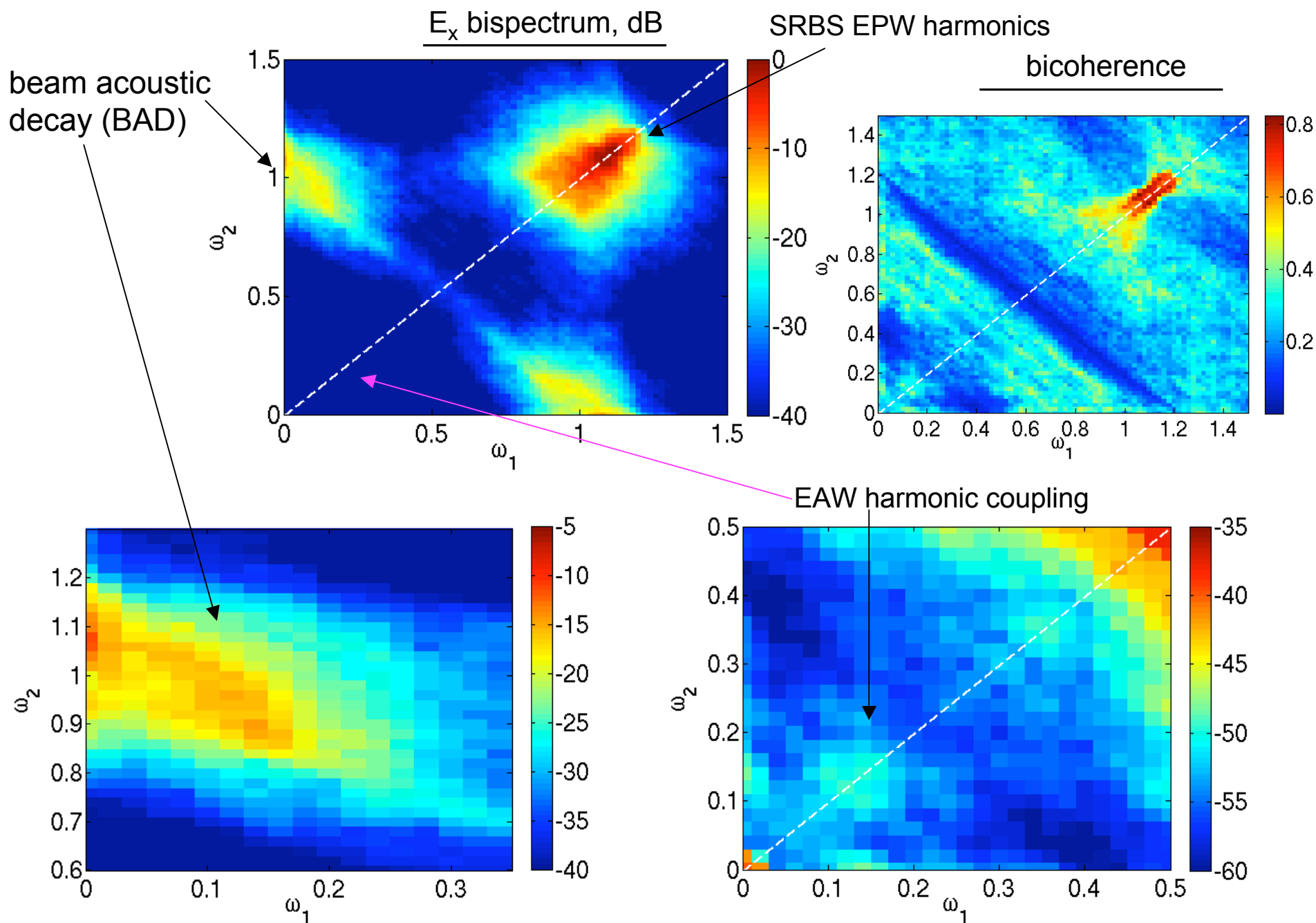
- bicoherence:
(normed bispectrum) $0 \leq |b_3| \leq 1$

$$b_3(\omega_1, \omega_2) = \frac{P_3(\omega_1, \omega_2)}{\sqrt{\langle |X(\omega_1 + \omega_2)|^2 \rangle \langle |Y(\omega_1)Z(\omega_2)|^2 \rangle}} = \frac{\text{phase-coupled power}}{\text{total power}}$$

Bispectrum of $E^+(\omega_1+\omega_2) E^-(\omega_1) E_x(\omega_2)$: SRBS, EATS ($I_0 = 2 \cdot 10^{15} \text{ W/cm}^2$)

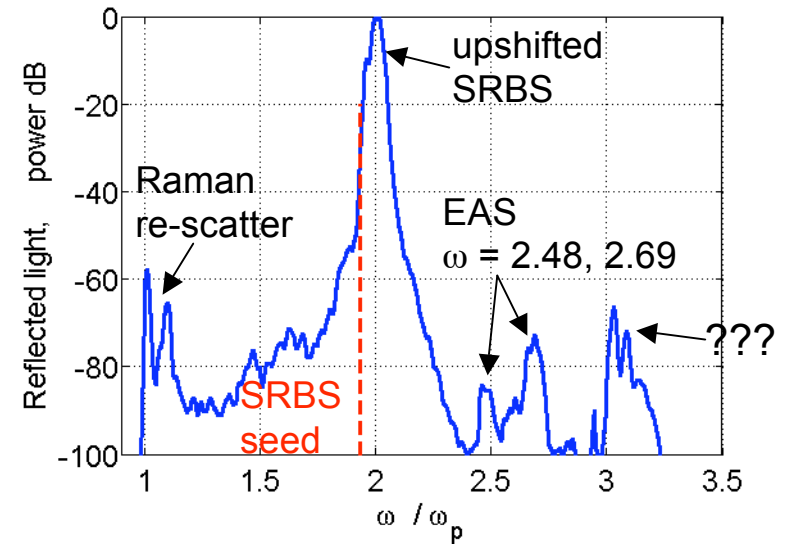
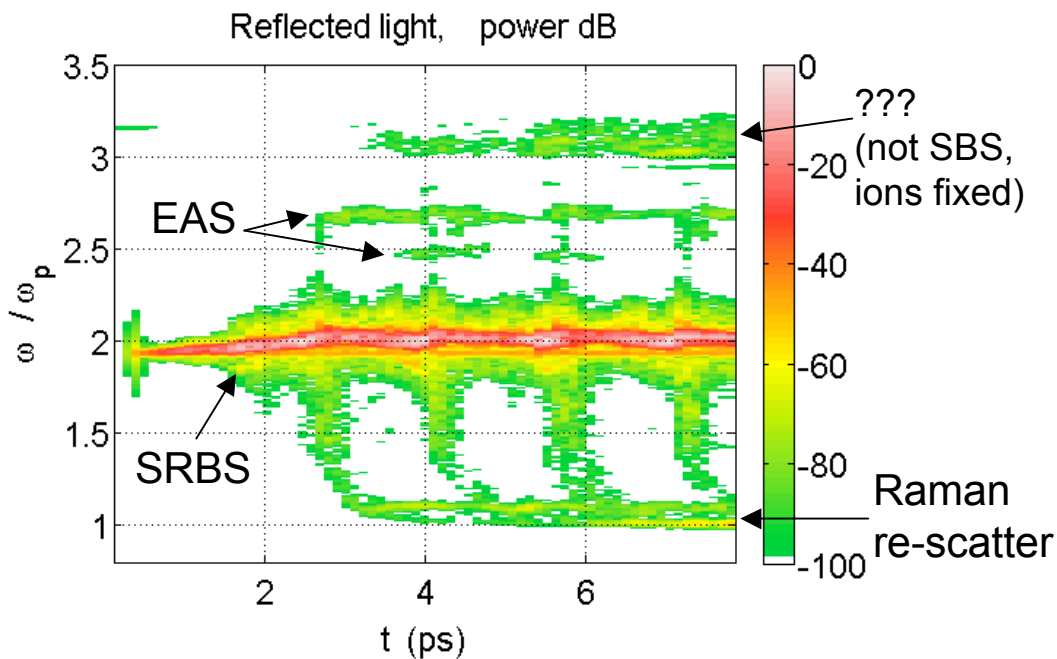
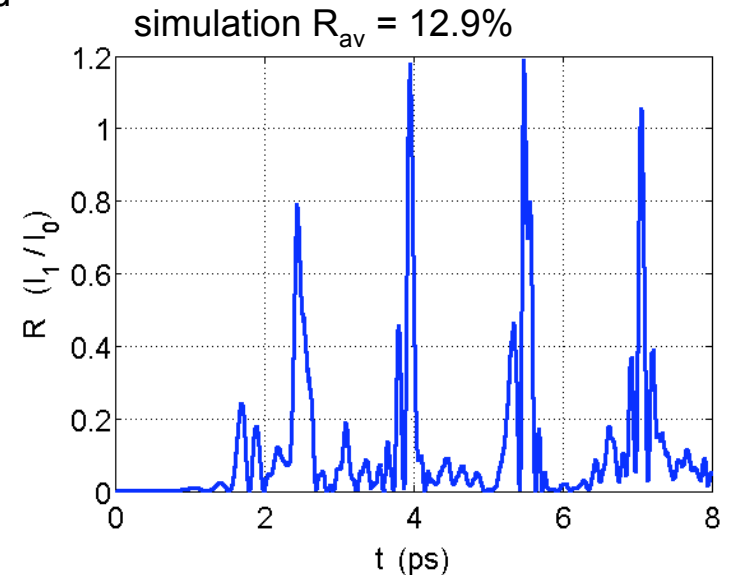
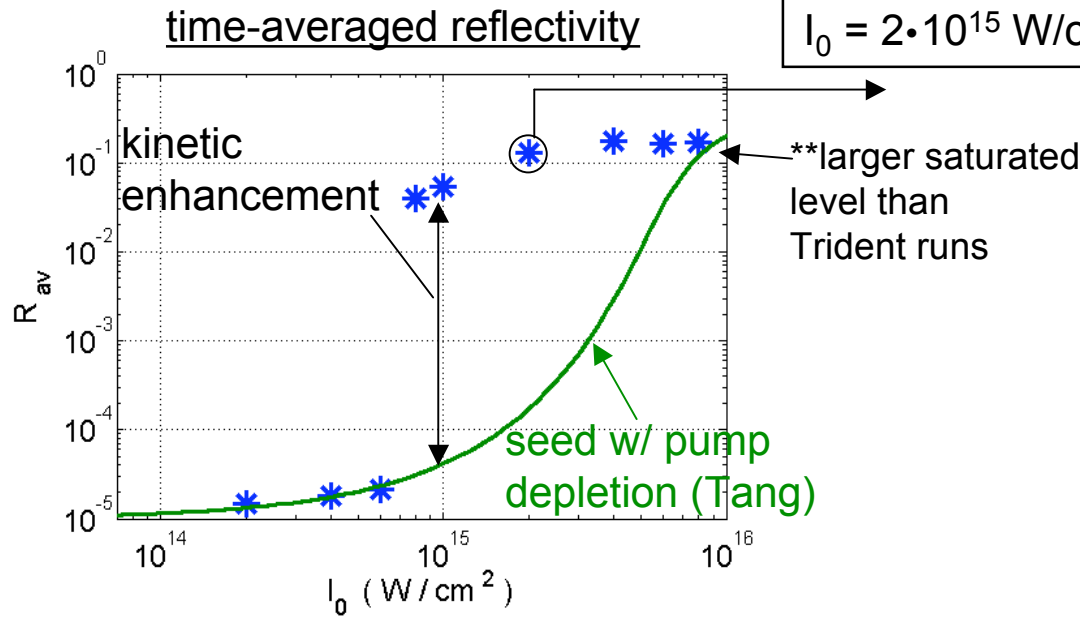


E_x Bispectrum: beam acoustic decay, EAW harmonics ($I_0 = 2 \cdot 10^{15}$ W/cm²)



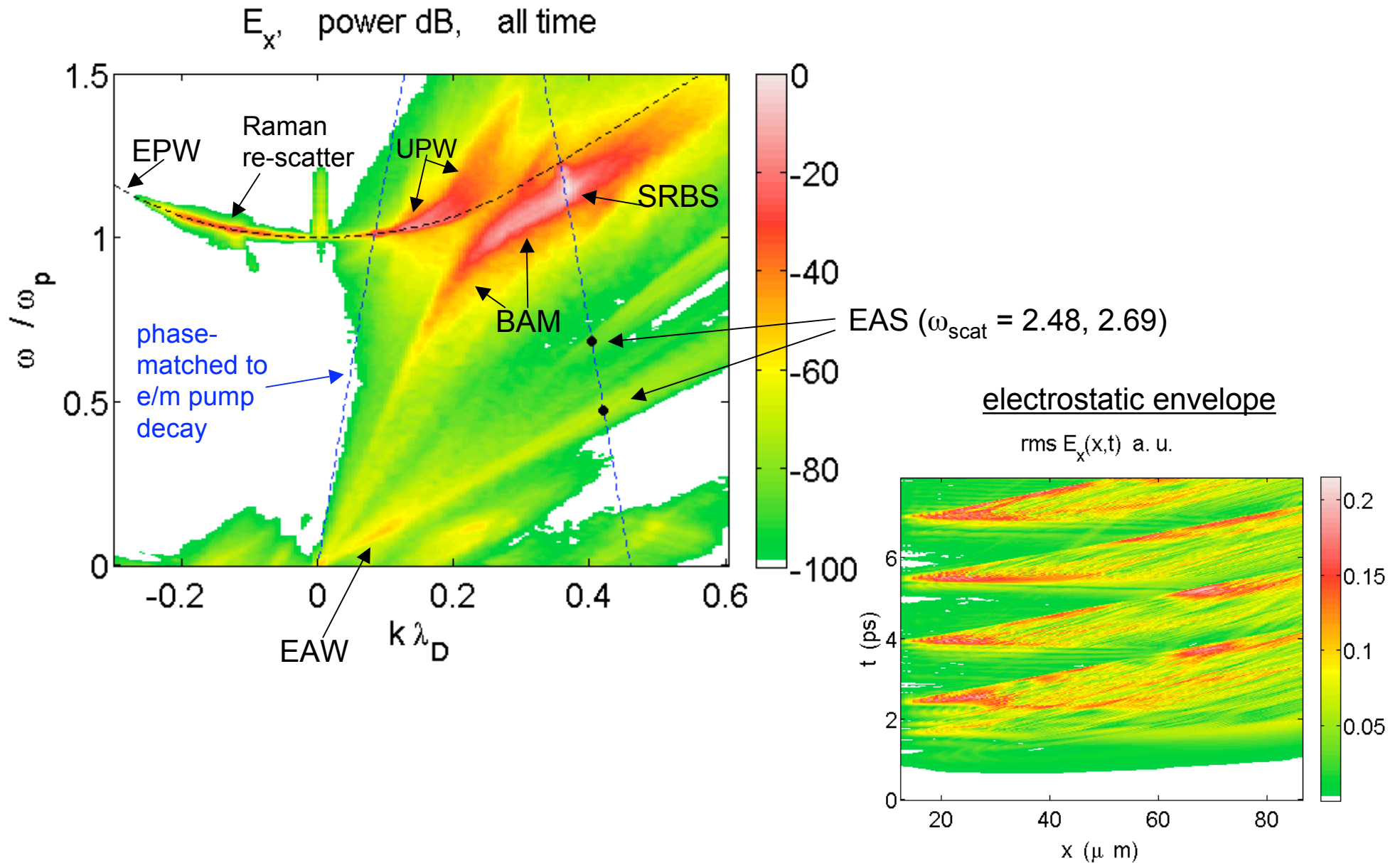
Hohlraum conditions: SRBS enhancement, EAW, EATS similar to Trident

$\lambda_{0V} = 351.3 \text{ nm}$, $n_e = 0.1 n_c$, $T_e = 3 \text{ keV}$, $\lambda_{1V} = 574.8 \text{ nm}$, $I_1 = 10^{-5} I_0$, $L_{\text{flat}} = 75.2 \text{ }\mu\text{m}$
 linear matching: EPW $k_2 \lambda_D = 0.357$
 amp. gain rate = $0.0190 \text{ }\mu\text{m}^{-1}$,
 intensity gain = 2.86, $R_{\text{av}} = 1.74 \cdot 10^{-4}$

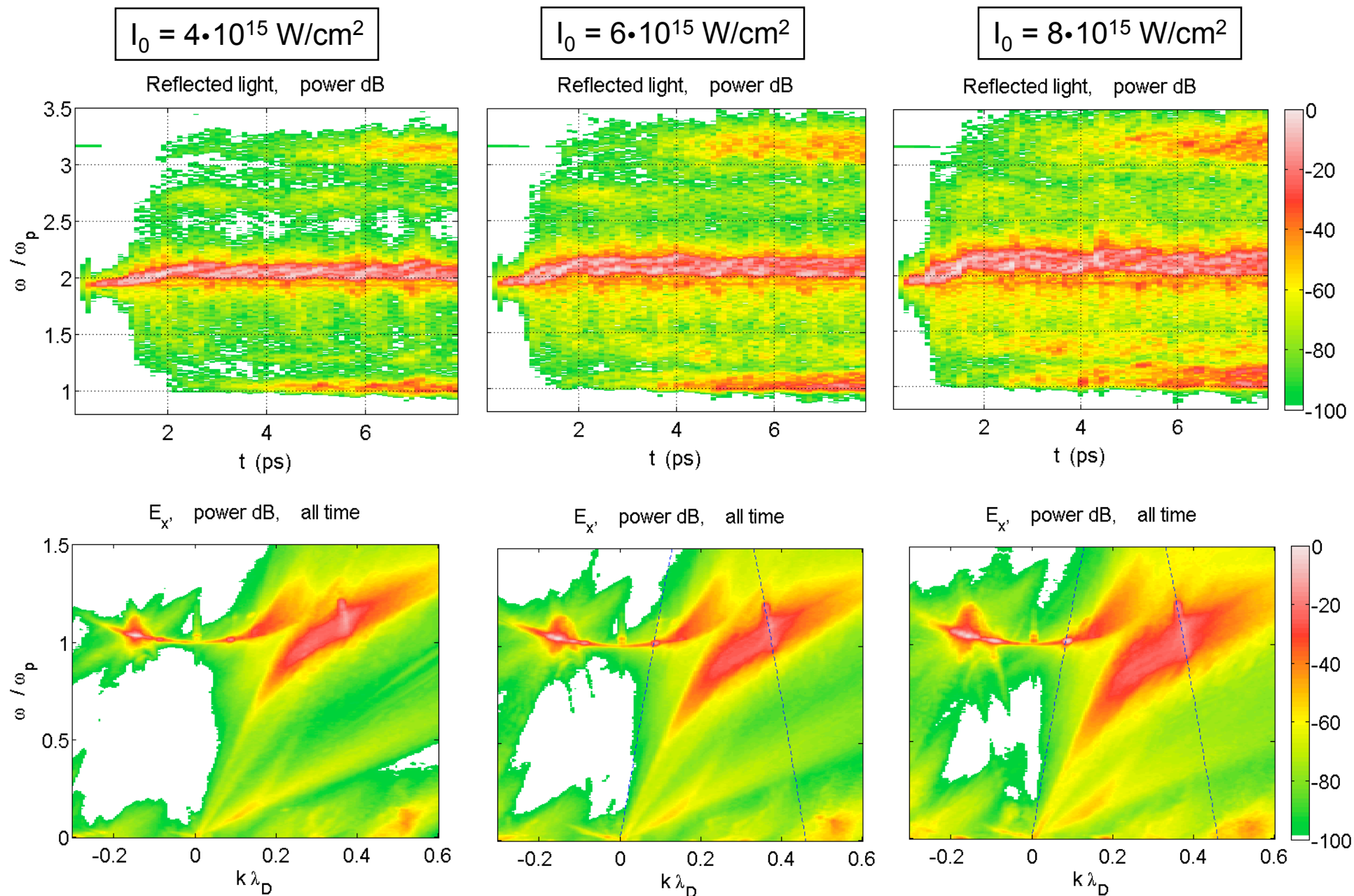


Hohlraum parameters: electrostatic activity shows EAW, BAMs, Raman re-scatter

$$I_0 = 2 \cdot 10^{15} \text{ W/cm}^2$$



Hohlraum parameters: BAD-EATS persists at higher pump strengths, but Raman re-scatter and mysterious $\sim\omega_0$ reflected light grow



Conclusions and future work

Conclusions

- Electron trapping leads to kinetically enhanced SRBS, plasmon frequency downshift.
- SRBS is bursty, frequency upshifted; EAS light also observed for moderate pump strengths.
- Beam acoustic modes (BAMs) and electron acoustic waves (EAWs) observed, both in Trident single-hot-spot and hohlraum fill conditions.
- Hermite projection: linear modes of numerical distribution contain BAMs, some of which are linearly unstable, and heavily-damped EAWs.
- EAWs are energized by beam acoustic decay (BAD): $BAM \rightarrow BAM + EAW$.
- Bispectrum supports phase-locked nature of BAD, EATS.

Future Work

- Threshold for kinetic enhancement: does a simple rule of thumb exist? Useful for designers.
- Experimental work: can EAWs, BAMs, EATS vs. SEAS mechanism be studied? EAS may be a miner's canary that (mild) kinetic enhancement is happening.
- Ions: Not shown here; early work shows BAMs, EATS survives (see Strozzi Ph.D thesis, 2005).
- What is the SBS-like scattering, and accompanying low-frequency electrostatic feature, in the hohlraum runs?

Reprints, comments, questions?
Leave name, email or physical address
